

Registration of a Ikonos image to a Digital Surface Model and true orthorectification

J.A. Gonçalves

Faculdade de Ciências, Universidade do Porto, Portugal

Keywords: IKONOS, Digital Surface Model, orthorectification

ABSTRACT: Ikonos images are provided with a set of coefficients of rational polynomial functions (RPC, rational polynomial coefficients) that are a numerical replacement of the exact sensor model equations. These functions derived from the approximate sensor exterior orientation, do an object to image projection with an accuracy of 10 meters. Image orientation improvements are usually done in image space by a simple translation or an affine transformation.

This paper presents a method of improving the image orientation using a Digital Surface model (DSM) of an urban area, in the form of 1 meter spacing grid, obtained by laser scanning. Top lines of buildings, extracted from the DSM, are projected onto the image space, using the given RPCs, and adjusted to fit the building position on the image. These lines act as standard ground control points.

The work was carried with an Ikonos image of the city of Porto and a laser scanning DSM. The new image orientation was very similar to the orientation achieved with a set of GCP's surveyed with GPS. The DSM was then used to orthorectify the image. Due to the double projection in occlusion areas, these had to be predicted, using the projection rays defined by the RPC equations and the DSM. These areas were then used to mask the orthoimage.

Finally the orthoimage was overlaid with GIS data in order to demonstrate the potential positional accuracy for large scale map updating.

1 INTRODUCTION

High resolution sensors on-board of satellites, such as Ikonos or Quickbird, provide data for a fast update of topographic databases. They are frequently used in the generation of orthoimage based maps, keeping the standards expected for map scales as large as 1:5000 (Jacobsen, 2003). They are of particular interest in urban areas, where large scale mapping is needed and, due to rapid changes, frequent map updates must be done. In order to provide positionally accurate data, images must be oriented with ground control points (GCP) and orthorectified with a digital elevation model (DEM).

Unlike conventional wide angle photogrammetric cameras, satellite sensors have very narrow fields of view, as is the case of Ikonos, with a field of 1 degree. Images acquired on a nadir viewing, over terrain with moderate relief may not need the orthorectification since relief displacement may be negligible. However, most of the times images are acquired with some across-track angle, in order to decrease the time delay for image acquisition. The relief displacement suffered by an object of height h , observed in a

zenital angle β , is given by $h \cdot \tan(\beta)$. For example for $\beta = 20^\circ$, a frequent inclination of Ikonos images, an elevation of 30 meters is displaced by 11 meters (or 11 pixels, due to 1 meter sampling in Ikonos panchromatic images), which is a very large displacement. A detailed and accurate DEM is required to provide planimetric correction of terrain effects at 1 meter accuracy.

A much more significant effect of the side looking geometry occurs in urban areas with buildings and other man-made or natural objects. Standard DEMs, derived from cartography, only represent the terrain and not other objects over it. In this case, significant displacements will remain in orthorectified images. An important consequence is that georeferenced vector data will not overlay correctly the image, originating difficulties in data interpretation. Automatic extraction of features from images, for example for automatic change detection, will neither provide appropriate results.

A Digital Surface Model (DSM), representing the elevation of the terrain and all other features, is required for the generation of true orthoimages. DSMs are now frequently available in urban areas. Laser scanning techniques, although still relatively expensive, provide very accurate and dense digital surfaces, with many applications in urban planning. These data sets are normally provided in the form of regular grids with 1 meter grid spacing and decimeter vertical accuracy. For example, in Portugal all major urban areas, in a total area of more than 1000 km², were surveyed by this method (Edinfor, 2006).

This paper deals with the integration of a regular grid DSM and an Ikonos panchromatic image, both with a spatial resolution of 1 meter. The reason to use the two data sets is essentially the generation of a true orthoimage. This procedure has been studied by several authors, mainly for aerial images (Amhar *et al.* (1998), Schickler and Thorpe (1998), Braun (2003), Kuzmin *et al.* (2004)). It comprises a prediction of occluded areas to mask the final product. The quality of the orthoimages generated in this way, require a very precise orientation of the image with respect to the surface model. In order to have a precise registration between both data sets it was decided to orientate the image using features extracted from the DSM, instead of using field survey GCPs.

An Ikonos image of the city of Porto, in Portugal, acquired on December 2001 and processed in the GEO mode, was used in this study. A DSM covering approximately 7 square km was provided by the Portuguese company Edinfor and was acquired by the German company Toposys in May 2001. Figure 1 shows a representation of the DSM and the portion of the Ikonos image corresponding to the same area.

The DSM is georeferenced in the local map projection (map coordinates Easting and Northing referred later as E and N) and local geodetic datum. Heights are relative to the geoid. In order to use the Ikonos sensor model, an appropriate conversion to WGS84 geodetic coordinates was done by a seven parameter transformation. Heights were converted to heights above the ellipsoid by adding the local geoid undulation, approximately 55 meters.

2 IMAGE ORIENTATION USING THE DSM

2.1 *Ikonos sensor model*

The precise orientation of any satellite image requires a sensor model that represents the geometry of the image formation process, by means of a relation between the object

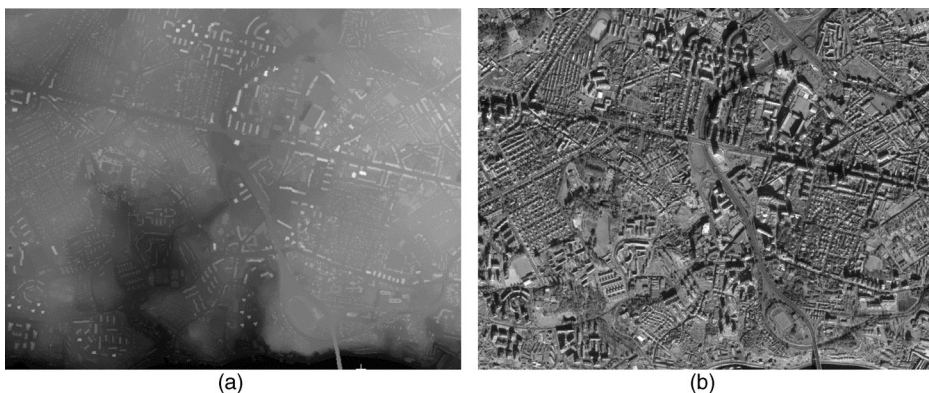


Figure 1. Representation of the DSM (a) and Ikonos panchromatic image (b).

space (3D) and the image space (2D). In the case of Ikonos the physical sensor model is not explicitly given. It is numerically replaced by a rational polynomial function, with polynomials of the 3rd degree. The image coordinates are generically expressed by equations:

$$x = \frac{P_1(\lambda, \varphi, H)}{P_2(\lambda, \varphi, H)} \quad y = \frac{P_3(\lambda, \varphi, H)}{P_4(\lambda, \varphi, H)} \quad (1)$$

where (λ, φ, H) are the WGS84 geodetic coordinates (object space) of a point and (x, y) the image coordinates in pixel units. Polynomials P_i are built with a total of 80 parameters (RPC, Rational Polynomial Coefficients) provided for each image. These formulas replace the physical sensor model, which includes the sensor position and attitude measured by on-board navigation equipment with very good accuracy. The object to image projection is done with errors of the order of 10 meters (Dial and Grodecki, 2002).

Orientation improvement is usually done in image space by a shift in image coordinates. Many authors describe in detail this simplified orientation model. See for example, Fraser and Hanley (2003) or Grodecki and Dial (2003). This is justified by the very good approximation of the initial image orientation and the very small field of view.

2.2 Ground control derived from the DSM

The image orientation is normally done with GCPs surveyed by GPS. In the present case a different approach was followed, making use of the DSM. First the DSM is represented in the form of a shaded relief image, allowing for a precise identification of roof edges. Some edges are digitized and then projected, taking into account the DSM heights, onto the image space. The projected lines are displaced from their actual position by a few meters, as expected, and the required shift in image space is determined by fitting the line to the roof edges on the image. Figure 2 shows a roof with digitised edges (a) and the corresponding edges projected on the image (b): initial position (displaced) and after moved to fit the edges.

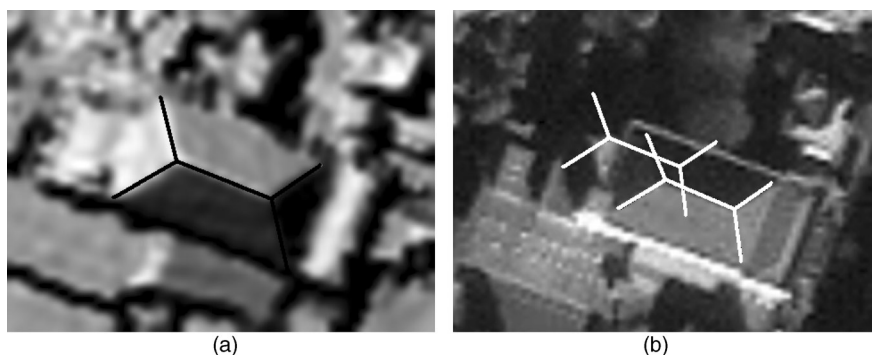


Figure 2. (a) Roof edges digitised on the shaded representation of the DSM; (b) edges projected on the image and after moved to their correct position.

This procedure was applied for a set of 9 locations distributed over the DSM area and shifts were carefully measured. Their statistics were calculated and are listed in Table 1. The shift is of the order of 10 pixels and could be determined with sub-pixel precision.

Applying the mean shift found, to equations (1), the image becomes correctly oriented, allowing for the generation of an orthoimage, using the DSM.

3 TRUE ORTHORECTIFICATION

The standard orthorectification procedure was applied, using software developed for that purpose. Each point of the DSM is projected onto the image space and a grey value is obtained by bilinear or cubic resampling, producing a rectified image with 1 meter pixel spacing. In the present case there are occluded areas, which should not be represented on the orthoimage. However, a well known effect of double projection occurs (Amhar *et al.* (1998), Schickler and Thorpe (1998), Braun (2003)). Points of buildings that are causing occlusions are projected onto their correct positions and on the occluded position, leading to a “ghost” effect. Figure 3 shows an example of this situation.

These occlusions must be predicted, by analyzing the DSM, and masked on the final orthoimage. A point is in a hidden area if the light ray that connects it to the sensor intersects the terrain surface in some other point. Local incidence direction must be

Table 1. Statistics of the shifts found in image coordinates of features projected from object space to image space.

	x (pixels)	y (pixels)
Mean	10.1	8.4
Standard deviation	0.6	0.6
Minimum	9.3	7.5
Maximum	11.0	9.6



Figure 3. (a) sample of the original Ikonos showing a tall building; (b) the same image after rectification with the DSM. The top of the building appears twice.

accurately known and can be easily determined using the corrected sensor model equations (1). These equations are inverted in order to calculate ground coordinates (E , N) for a given image position (x , y) and terrain height (h). The image to object projection can be expressed in generic terms by equation (2):

$$(E, N) = \mathbf{F}(x, y, h) \quad (2)$$

Considering two different heights, h_1 and h_2 (for example the minimum and maximum values of the DSM), two points are obtained. They define the local look direction vector. The azimuth, α , and elevation, β , can be easily calculated. These angles have a very small variation along the image due to the very small field of view of the sensor. For the image used, in the area of the DSM, the values of α and β , had mean values of 201.7 and 69.5 degrees and ranges of 0.26 and 0.30 degrees, respectively.

For any point of the DSM, P_0 with coordinates (E_0, N_0, h_0) , the angles α_0, β_0 are calculated as well as the corresponding unit vector. The equation of the light ray in the vector form can be written as:

$$(E_L, N_L, h_L) = (E_0, N_0, h_0) + \mu \cdot (\cos \beta_0 \sin \alpha_0, \cos \beta_0 \cos \alpha_0, \sin \beta_0) \quad (3)$$

where (E_L, N_L, h_L) are the coordinates of a point on the line and μ is a distance parameter. Figure 4 represents this situation: for a given point, P on the line the height of the point is compared to the height given by the DSM for position (E_L, N_L) . If the height of the line is smaller, then the point is hidden. Point P moves from P_0 to the maximum height of the DSM, with a small step in order to determine the point visibility.

All the DSM points are tested in order to determine the hidden area mask. Figure 5 shows a sample of the mask image generated for the DSM of Porto. In the whole DSM area a total of 5.6% of the pixels were in occluded areas.

The Ikonos image was orthorectified for the whole DSM area. The hidden area mask was then applied to the orthoimage. It covers the “ghost” effects found for the buildings that cause occlusions. Figure 6 shows an example of this situation.

The present case of processing a single image of the area is not as favorable as when orthorectifying conventional aerial photography with standard overlap factors. In the

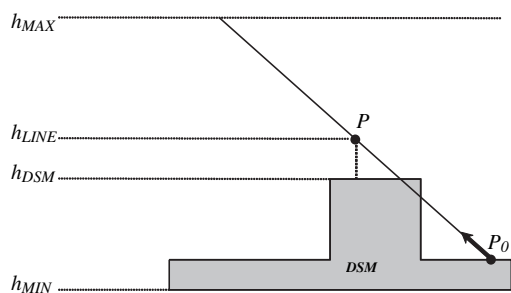


Figure 4. Procedure to determine visibility of point P_0 of the DSM.



Figure 5. Hidden area mask calculated from the DSM, taking into account the local viewing angle of the Ikonos image.

latter case, the pixels in the mask of a given image are probably visible on some other image. These areas can be filled with data from other images. In our case there is no other solution but leaving the mask. Further processing of the orthoimage, such as for example segmentation or classification of multispectral bands (fused to the panchromatic) must take into account the existence of the mask.



Figure 6. Small portion of the ortho image before (a) and after (b) the application of the mask.

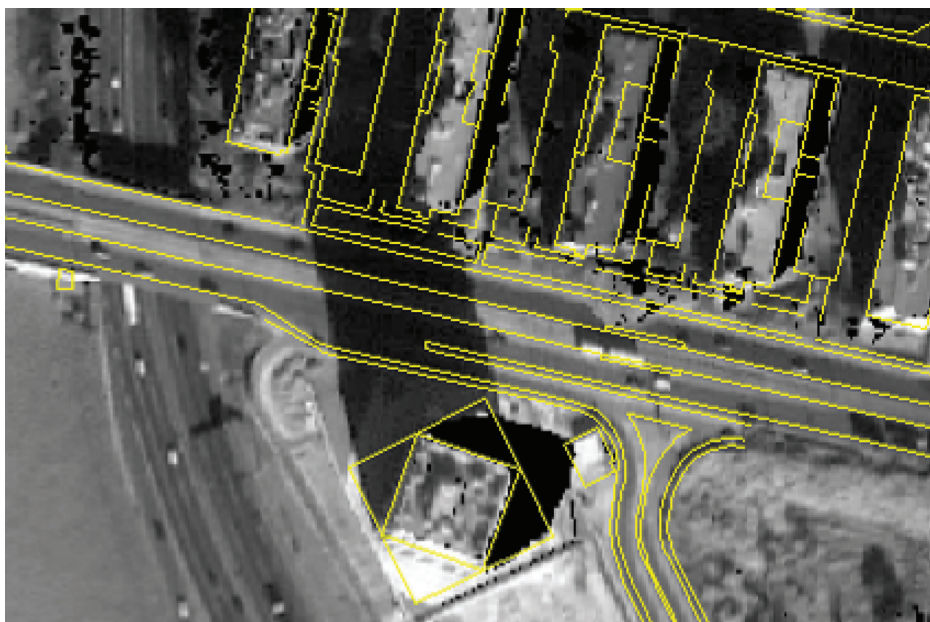


Figure 7. Small portion (320 m by 185 m) of the ortho image with overlaid vector data.

Finally, in order to independently assess the planimetric accuracy of the orthoimage, a vector map (of nominal scale 1:1000) was overlaid. The coincidence of buildings is in general very good, as can be seen in Figure 7.

4 CONCLUSIONS

High resolution images are useful for fast map updating, especially in urban areas. Quite often images are acquired with relatively large incidence angles, leading to strong relief effects in high buildings. Laser scanning DSMs, can be used to generate true orthorectified images.

Two aspects of the combination of a DSM and an Ikonos image were analyzed. The first was the orientation of the image with edges extracted from the DSM. This method not only gave a very good precision (sub-pixel) as also avoided the field survey of ground control points.

The second aspect was the application of a true orthorectification of buildings in urban areas. Large relief displacements in high resolution satellite images acquired with side looking angle are quite inconvenient and can be reasonably removed by this method. The procedure is relatively simple and straightforward. There is the limitation that masked areas will remain if a single image is treated but further image analysis, for example by overlaying GIS vector data, is much more rigorous.

REFERENCES

- Amhar, F., Jansa, J., and Ries, C. 1998. The generation of true orthophotos using a 3d building model in conjunction with a conventional DTM. *International Archives of Photogrammetry and Remote Sensing*, 32(4) pp. 16–22.
- Braun, J. 2003. Aspects on True-Orthophoto Production. In Fritsch (Ed.): *Photogrammetric Week '03*, Wichmann Verlag, Heidelberg (2003), pp. 205–214.
- Dial, G. and Grodecki, J. 2002. Block Adjustment with Rational Polynomial Camera Models. *Proceedings of ASPRS 2002 Conference*, Washington, DC.
- Edinfor, 2006. <http://www.it-geo.pt>, last visited in 2006.
- Fraser, C. and Hanley, H. 2003. Bias Compensation in Rational Functions for Ikonos Satellite Imagery. *Photogrammetric Engineering & Remote Sensing*, 69(1): 53–57.
- Grodecki, J. and Dial, G. 2003. Block Adjustment of High-Resolution Satellite Images Described by Rational Polynomials. *Photogrammetric Engineering & Remote Sensing*, 69(1): 59–68.
- Jacobsen, K. 2003. Geometric Potential of IKONOS and QuickBird Images. In: Fritsch (Ed.): *Photogrammetric Week '03*, Wichmann Verlag, Heidelberg (2003) pp. 101–110.
- Kuzmin, Y., Korytnik, S., Long, O. 2004. Polygon-based True Orthophoto Generation. *International Archives of Photogrammetry and Remote Sensing*. Vol. 35, part B4, p. 529.
- Schickler, W. and Thorpe, A. 1998. Operational procedure for automatic true orthophoto generation. *International Archives of Photogrammetry and Remote Sensing*, 32(4), pp. 527–532 (1998).
- Zhan, Q., Shi, W. and Xia, Y. 2005. Quantitative analysis of shadow effects in high resolution images of urban areas. *International Archives of Photogrammetry and Remote Sensing*, Vol 36, (8/W27).